2003

Evaluation of the CERC Formula Using Large-Scale Laboratory Data

Ernest R. Smith
U.S. Arm y Engineer Research and Developm ent Center, smithe@wes.army.mil

Ping Wang
University of South Florida, pwang@usf.edu

Jun Zhang
Texa s A&M University

EVALUATION OF THE CERC FORMULA USING LARGE-SCALE MODEL DATA

Ernest R. Smith[1], Ping Wang[2], Jun Zhang[3]

Abstract: Longshore transport experiments were conducted in a large-scale physical model to evaluate predictions of the CERC formula with measured longshore sediment transport rates. It was found that the CERC formula produced reasonable estimates if the coefficient *K* was calibrated and applied to waves with similar breaker type. The calibrated *K* values are much smaller than values that are commonly used, and there appears to be a strong dependency of transport rate on breaker type. Additional comparisons were made with the formula proposed by Kamphuis (1991). The Kamphuis equation, which includes wave period, a factor that influences breaking, gave good estimates. Examination of the cross-shore distribution of longshore sediment transport indicates that there are three distinct zones of transport: the incipient breaker zone, the inner surf zone, and the swash zone, with each zone contributing a different fraction to the total transport rate. Transport in the incipient breaker zone was influenced by breaker type, transport in the inner surf zone was controlled by depth, and transport in the swash zone showed dependencies on wave height and, in particular, wave period. Swash zone transport was found to have a significant contribution to the total transport rate.

INTRODUCTION

Total longshore sediment transport rate and its cross-shore distribution in the surf zone are essential to many coastal engineering and science studies. Practical engineering applications such as beach response in the vicinity of coastal structures, beach-fill evolution and re-nourishment requirements, and sedimentation rates in navigation channels all require accurate predictions of longshore sediment transport rates. To maintain navigable waterways along U.S. coasts, the U.S. Army Corps of Engineers regularly applies analytical and numerical models to estimate the total longshore sediment transport rate and its cross-shore distribution in the surf zone. Present predictive tools have been developed based primarily on field studies; however, obtaining high-quality data in the field is difficult (Wang and Kraus, 1999). Arguably the most widely used model for estimating total longshore sediment transport rate is the "CERC" formula (*Shore Protection Manual*, 1984). The model, based on the assumption that the total longshore sediment transport rate is proportional to longshore energy flux, is given as:

$$Q = \frac{K}{16\sqrt{\gamma_b}} \rho g^{\frac{3}{2}} H_{sb}^{\frac{5}{2}} \sin(2\theta_b) \tag{1}$$

in which Q is the submerged total longshore transport rate, K is an empirical coefficient, ρ is density of water, g is acceleration due to gravity, H_{sb} is significant wave height at breaking, γ_b is the breaker index, and θ_b is wave angle at breaking. The Shore Protection Manuals recommends a value of K of 0.39, which was derived from the original field study of Komar and Inman (1970) using sediment

1) U.S. Army Engineer Research and Development Center, Coastal and Hydraulics Laboratory, 3909 Halls Ferry Road, Vicksburg, MS 39180, USA. smithe@wes.army.mil
2) Department of Geology, University of South Florida, 4202 E. Fowler Avenue, Tampa, FL. 33620, USA. pwang@chuma1.cas.usf.edu
3) Coastal and Ocean Engineering Division, Texas A&M University, College Station, TX, 77843 USA. jzhang@civilmail.tamu.edu

tracers. However, the expression is best used if the coefficient is calibrated using data for a particular site. For design applications with adequate field measurements, the CERC formula can be calibrated and applied to estimate total longshore sediment transport rates with reasonable confidence ($\pm$ 50 percent). However, many sites do not have transport data available to calibrate *K*, and for design applications without calibration data the CERC formula provides only order-of-magnitude accuracy (Fowler et al., 1995; Wang et al., 1998). The recommended value of $K = 0.39$ has been commonly used to represent the potential longshore transport rate. However, Miller (1998) found that the CERC formula sometimes over and sometimes under predicted longshore transport rate for measurements during storms, indicating the value of *K* also can be higher than 0.39.

Most of the data available for calibration of empirical longshore sediment transport formulas were obtained from field measurements. Field measurements in the dynamic surf zone are non-controllable and non-repeatable, which may lead to large uncertainties (Schoonees and Theron, 1993, 1994; Wang et al., 1998; Wang and Kraus, 1990). In addition, only a limited number of parameters can be measured in the field with coarse temporal and spatial resolutions.

The few laboratory studies on longshore sediment transport are advantageous in that they are controllable and repeatable, and therefore, should be more accurate than field data. Laboratory data have not been broadly used in the calibration of longshore transport formulas, largely because typically small scales were used. However, Kamphuis (2002) found that experiments conducted with a relatively small model had little scale effect and uncertainties were less than that of field results. Kamphuis suggests that it is difficult to improve estimates of longshore sediment transport rate based solely field data because of large uncertainties associated with measuring basic variables and the subjectivity of interpreting results. Kamphuis concludes that any improvements to sediment transport relationships need to be developed from controlled and controllable model tests, despite the shortcomings of physical models.

Kamphuis (1991) developed a relationship for estimating longshore sediment transport rates based primarily on physical model experiments. The equation, which Kamphuis (2002) found to be applicable to both field and model data, is expressed as:

$$Q_u = 2.27 H_{sb}^2 T_p^{1.5} m_b^{0.75} d_{50}^{-0.25} \sin^{0.6}(2\theta_b) \tag{2}$$

in which Q_u is the transport rate of underwater mass in kg/s, T_p is the peak wave period, m_b is the beach slope from the breaker line to the shoreline, and d_{50} is the median grain size. Kamphuis (2002) redefines the beach slope as the slope that causes breaking, i.e., the slope over one or two wavelengths offshore of the breaker line. In the present study, the Kamphuis (1991) version was used because of difficulty in defining the slope offshore of breaking. Equation 2 is appealing because it includes wave period, which influences wave breaking (Galvin, 1968), and grain size diameter, a relevant factor in incipient sediment motion.

Research is ongoing in a large-scale physical model to improve present predictive equations for longshore sediment transport. The purpose of this paper is to compare estimates from Equations 1 and 2 to measurements obtained in the model. The CERC formula, specifically the coefficient *K*, will be evaluated based on the comparison.

PHYSICAL MODEL DESCRIPTION

Experiments were conducted in the Large-scale Sediment Transport Facility (LSTF) of the US Army Engineer Research and Development Center's Coastal and Hydraulics Laboratory. The LSTF is a large-scale laboratory facility, 30-m wide, 50-m long, 1.4-m deep, and is capable of simulating conditions comparable to low-energy coasts (Figure 1). The intent of the facility is to reproduce surf zone processes found on a long, straight, natural beach in a finite-length basin, and improve existing methods for calculating total longshore sediment transport rate and its cross-shore distribution. Hamilton and Ebersole (2001) found the LSTF was capable of producing uniform and steady hydrodynamic parameters that drive longshore sediment transport. The LSTF provides a controllable environment for accurate measurements of longshore sediment transport rate and its cross-shore distribution (Wang et al., 2002a).

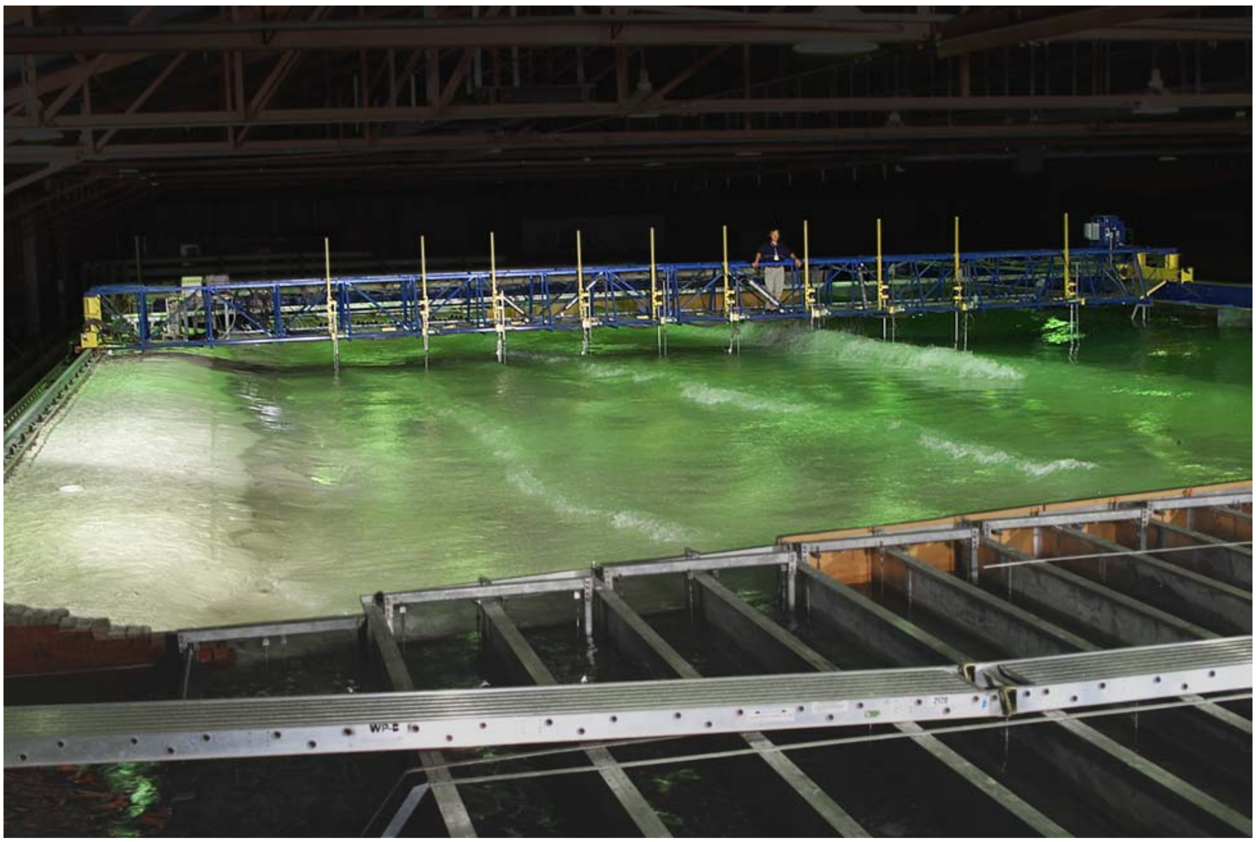

Fig. 1. An experiment in the LSTF

Four wave generators are used to produce waves in the LSTF. Each generator has a board length of 7.62 m and is synchronized with the other generators to produce 30.5-m long unidirectional long-crested waves at an incident wave angle of 10 deg to shore normal. The wave makers can produce maximum wave heights of 0.5 m.

The sand beach consists of approximately 150 m^3 of fine quartz sand with d_{50}, = 0.15 mm. The beach was approximately 0.25-m thick, extended 27 m alongshore, 18 m offshore, and was constructed to a trapezoidal planform shape to correspond to the incident wave approach. To minimize longshore variation in waves and currents, it was necessary to maintain straight and parallel contours throughout the beach. Beaches having three-dimensionality affect incident waves and, subsequently, the longshore currents and sediment transport associated with the waves.

To minimize adverse laboratory effects created by the boundaries of the finite-length beach, wave-driven currents were supplemented by an external recirculation system (Hamilton et al., 2001, Hamilton and Ebersole, 2001, and Visser, 1991). The recirculation system consisted of 20 independent vertical turbine pumps placed in the cross-shore direction at the downdrift boundary. Flow channels placed upstream of each pump were used to direct flow to the pump, which externally re-circulated water to the upstream end of the facility where it was discharged through flow channels onto the beach. The objective of this system is to maximize the length of beach over which waves and wave-driven longshore currents are uniform by continually re-circulating currents of the same magnitude as the mean wave-driven longshore current through the lateral boundaries of the facility. Each pump includes a variable speed motor to control discharge rates, which allows variation in the cross-shore distribution of longshore current.

The facility includes a 21-m-long instrumentation bridge that spans the entire cross-shore of the beach. The bridge serves as a rigid platform to mount instruments and observe experiments. Each end of the bridge is independently driven on support rails by drive motors, which allows it to travel the entire length of the wave basin. The bridge can be driven either at the bridge or remotely by entering the desired longshore (Y) location on a PC in the LSTF control room.

Time series of water surface elevations were measured using single-wire capacitance-type wave gauges. Ten gauges mounted on the instrumentation bridge measured wave heights as they transform from offshore to nearshore. Additionally, a gauge was placed in front of each wave generator to measure offshore wave characteristics.

Ten acoustic Doppler velocimeters (ADVs) were used to measure the total velocities (wave orbital velocities and unidirectional longshore currents). The ADVs were positioned at the same cross-shore position on the bridge with the wave gauges, but separated by approximately 40 cm in the longshore direction to prevent interference between the two instruments. All of the ADVs sample at a point, but were mounted on vertical supports so that the vertical position of the sampling volume to be adjusted. Typically, the ADVs were positioned vertically to sample at a location that gives the approximate average velocity in the water column (an elevation equal to one third of the water depth from the bottom, Hamilton et al., 2001).

Sediment flux was obtained from twenty 0.75-m wide traps located at the downdrift boundary, which encompassed the entire surf zone. Eighteen traps were installed in the downdrift flow channels and two additional traps were located landward of the first flow channel to quantify longshore sediment transport rate near the still-water shoreline and in the swash zone. Each sand trap is equipped with three load cells to weigh the amount of trapped sand, to determine the cross-shore distribution of longshore sediment transport.

EXPERIMENTS AND RESULTS

Total Longshore Transport Rate

The first step of each experiment was to determine the distribution of wave-induced longshore current and to properly adjust the re-circulation pumps. Visser (1991) determined from laboratory experiments that if the re-circulated (pumped) currents either exceeded or were less than the wave-driven currents, an internal current would develop and re-circulate within the offshore portion of the basin. Visser also found that as the pumped currents approached the proper (wave-driven) current, the internally re-circulated current was minimized. Therefore, it was desired to match wave-driven currents with pumped currents. Initial pump settings were based on results of the numerical models NMLONG (Kraus and Larson, 1991) and NEARHYDS (Johnson, 2003). The iterative approach described by Hamilton and Ebersole (2001) and Hamilton, et al. (2001) was used to determine the optimum pump settings. After the beach had evolved to an equilibrium or quasi-equilibrium profile, and the pumped currents matched measured velocities, experiments on longshore transport rate were initiated.

Irregular incident wave conditions were designed to obtain and compare longshore transport rates for different breaker types. Four conditions generated in the LSTF are listed in Table 1, where H_{mo} is the energy-based significant wave height measured near the wave makers. Each test was conducted with a water depth, h, of 0.9 m at the wave generators.

Table 1. Longshore Sediment Transport Experiment Wave Conditions

Experiment Number	Breaker Type	H_{mo} m	H_{sb} m	T_p s	h m	θ_b deg	γ_b	m_b
1	Spilling	0.25	0.26	1.5	0.9	6.5	0.57	0.035
3	Plunging	0.23	0.27	3.0	0.9	6.4	0.96	0.023
5	Spilling	0.16	0.18	1.5	0.9	6.7	0.29	0.021
6	Plunging	0.19	0.21	3.0	0.9	6.4	0.58	0.023

Determination of H_{sb} for irregular waves is somewhat subjective. In the present study, the main breaker line was determined as the location landward of which significantly accelerated rate of wave-height decay was measured. This criterion was based on the comprehension that a dramatic wave-energy loss, and therefore, wave height decrease, should follow dominant wave breaking. Visual observations during the experiments supported the above determination.

Wave height distribution and the average profile associated with each experiment are shown in Figures 2 through 5. Waves broke by spilling during Test 1, and Figure 2 shows a gradual decay of wave height through the surf zone, with incipient breaking occurring approximately 13 m from the shoreline. The beach profile is near planar inside the surf zone. Figure 3 shows the distribution of wave heights and profile associated with Test 3. Test 3 waves shoaled to a height of 0.27 m and sharply decreased at approximately 13 m from the shoreline. Wave heights are similar to those of Test 1 in the inner surf zone. Test 3 waves broke by plunging as evident by the breakpoint bar and trough formed at approximately 11 m. Test 5 waves show a very gradual decrease across the surf

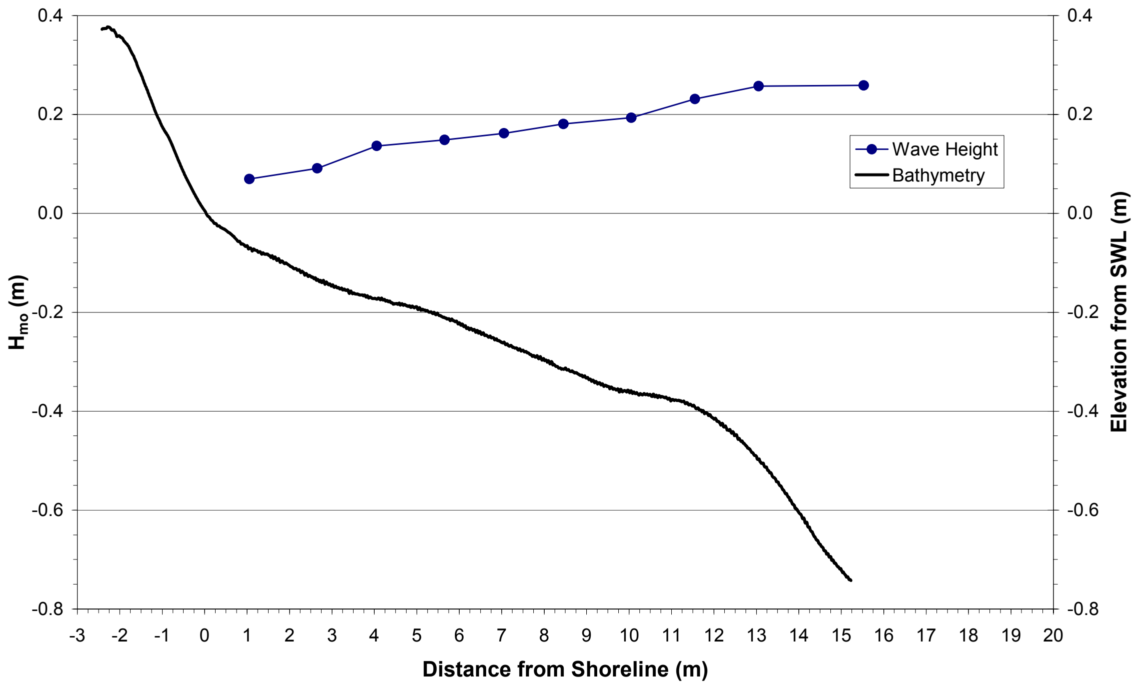

Fig. 2. Wave height distribution and beach profile associated with Test 1

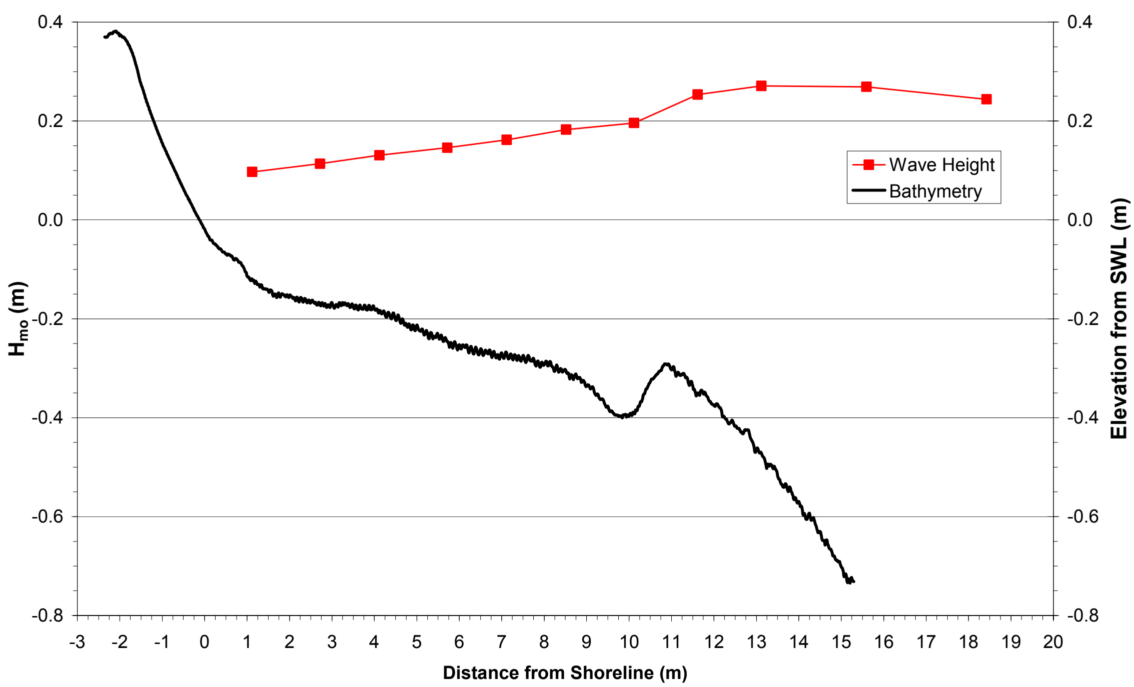

Fig. 3. Wave height distribution and beach profile associated with Test 3

zone 16 m from the shoreline (Figure 4). In this case, inner surf zone wave height is significantly less than observed for Tests 1 and 3. The average beach profile of Test 1 was used as the initial profile for Test 5, and little change occurred between the two profiles. During Test 5, erosion occurred shoreward of 9 m from the shoreline and sand was deposited between 10 and 12 m from shore, and seaward of 13 m. Figure 5 shows wave transformation and the beach profile formed during Test 6. Waves shoaled to 0.21 m, 12 m from the shore, where heights sharply decreased. Wave heights in the inner surf are similar to those of Test 1 and Test 3. A subtle breakpoint bar formed under the plunging wave conditions.

Total longshore transport rate was computed by summing the sediment flux measured in all of the traps. Measured transport rates are given in Table 2 along with the predicted values from Equations 1 and 2. If the recommended *K*-value of 0.39 is used, the CERC formula (Equation 1) over-predicts measured values from the spilling cases by a factor of 8 for Test 1 and nearly 7 for Test 5. Estimates are greater than a factor of 3 for both plunging wave cases. The CERC formula produced similar estimates for Test 1 and Test 3 because they have similar wave heights, although breaker types differed. Measured transport rates were nearly 3 times greater for Test 3 (plunging) than Test 1 (spilling). Results using Kamphuis (1991) (Equation 2) produced more consistent estimates with the measured data; differences ranged between one percent for Test 1 to 25 percent for Test 5. The improved estimates of Kamphuis (1991) can in part be attributed to the incorporation wave period into Equation 2, which influences breaker type.

Table 2. Comparison between measured and predicted total longshore transport rate

Experiment Number	Measured m^3/yr	CERC Formula (K=0.39) m^3/yr	Kamphuis (1991) m^3/yr
1	2,660	22,030	2,680
3	7,040	23,850	5,920
5	1,170	7,940	880
6	3,410	12,770	3,410

The results indicate that in addition to wave height, breaker type is a factor in estimating longshore transport rates. Kraus et al. (1982) identified four different cross-shore distribution patterns of longshore sediment transport from field measurements. Sunamura and Kraus (1985) commented that the wave conditions during the experiment were a combination of spilling and plunging breaker types.

Considering the role of breaker type in longshore transport rates, the CERC formula was evaluated based on breaker type. If measured transport rates from Test 1 are used to calibrate the CERC formula, $K = 0.049$. Applying this coefficient to the wave conditions of the lower energy spilling case (Test 5) gives a transport rate of 1060 m^3/yr, or a 9 percent difference from the measured rates. Likewise, if the CERC formula is calibrated using transport rates from Test 3, $K = 0.119$. Applying this coefficient with wave conditions of the lower energy plunging case (Test 6), a transport rate of 3760 m^3/yr is calculated, which is 10 percent of measured rates. The

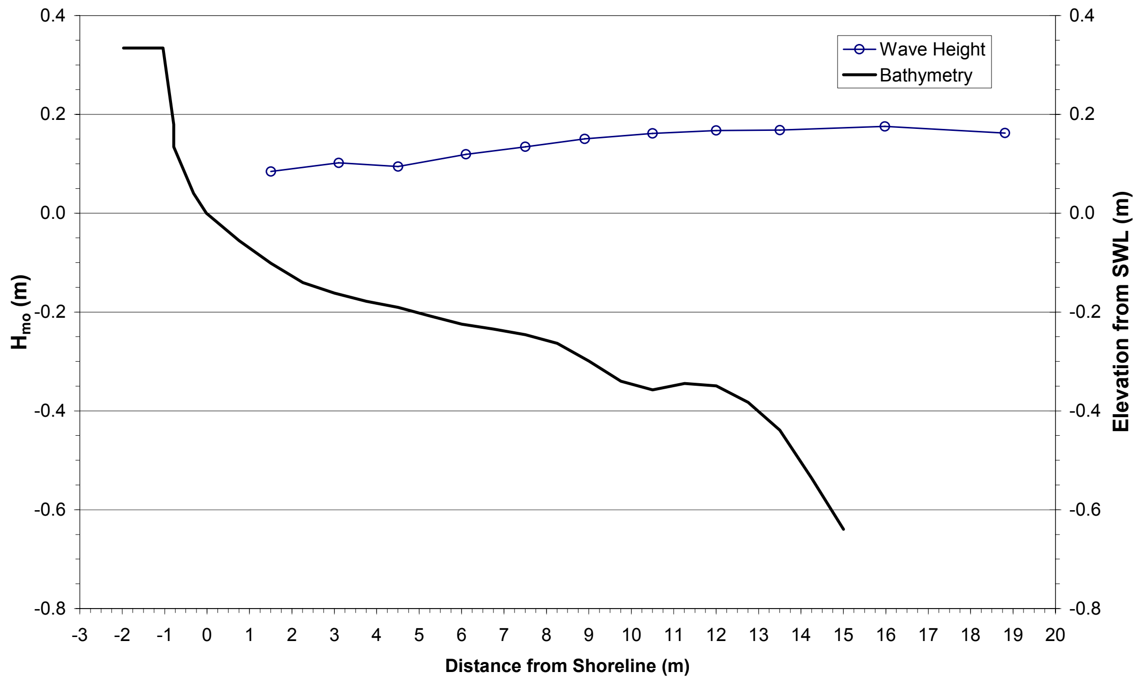

Fig. 4. Wave height distribution and beach profile associated with Test 5

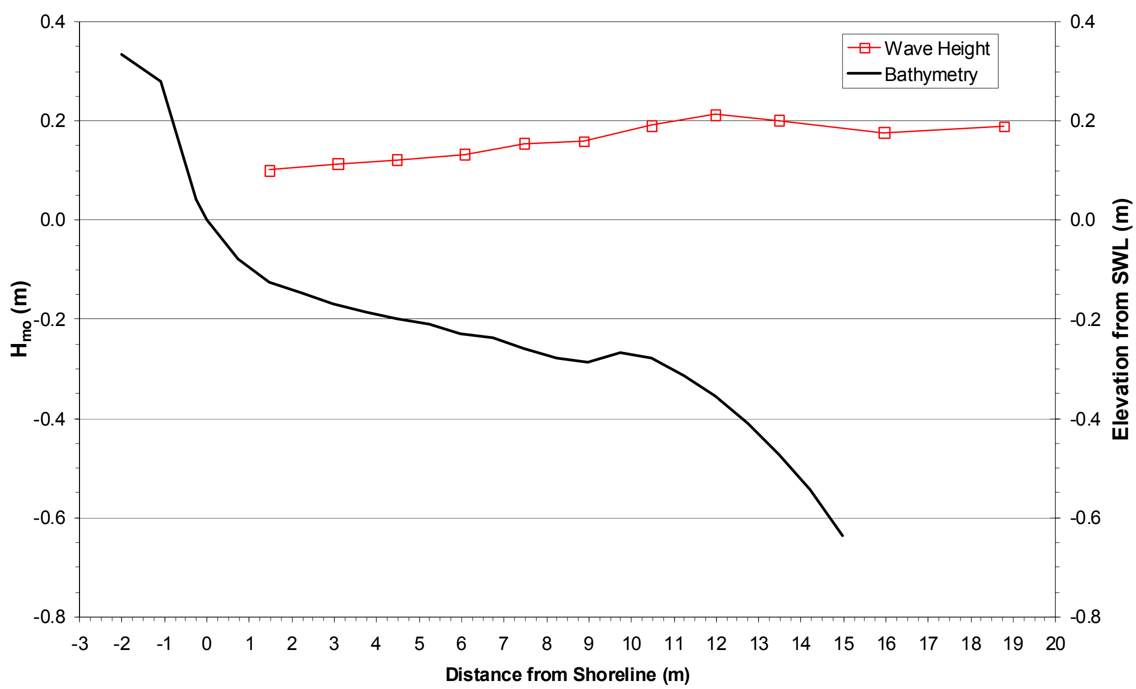

Fig. 5. Wave height distribution and beach profile associated with Test 6

improved rates are illustrated in Figure 6, which shows calculated versus measured transport rates using the CERC formula with calibrated *K*-values. Additionally, CERC formula estimates using $K = 0.39$ and estimates from Kamphuis (1991) are included. The figure indicates that the Kamphuis equation, which includes wave period, which influences breaker type, predicts measured rates well, and the CERC formula gives reasonable estimates if *K* is calibrated, and it is applied to similar breaker types.

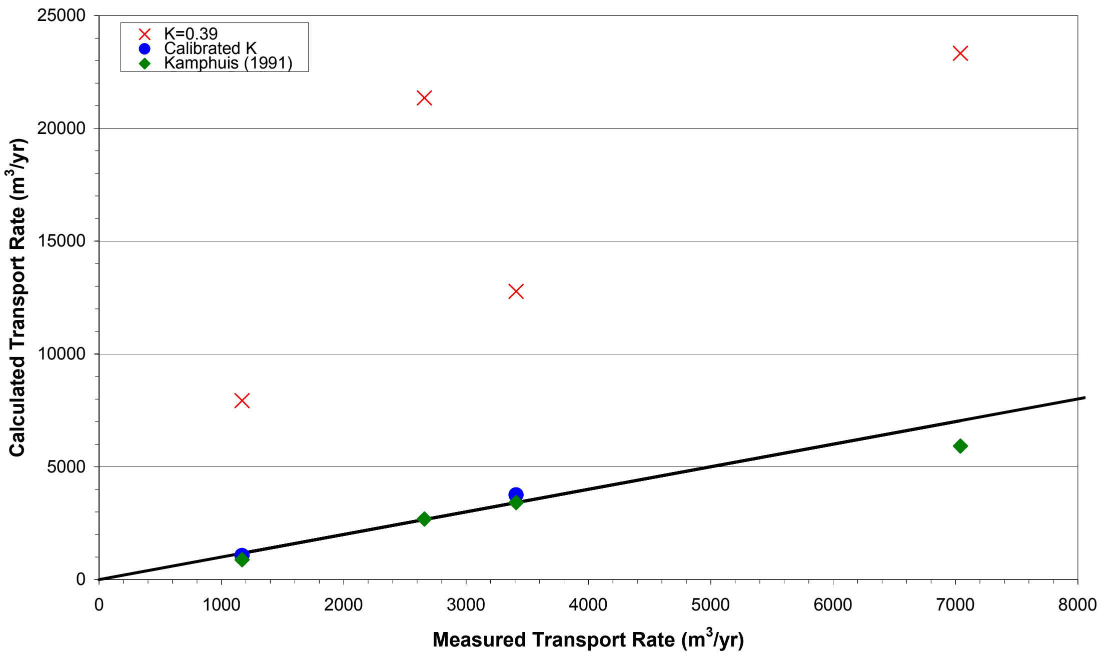

Fig. 6. Comparison of calculated to measured transport rates

Cross-Shore Distribution Of Longshore Transport Rate

Ongoing research in the LSTF includes investigation of the cross-shore distribution of longshore sediment transport. Longshore sediment flux was calculated from the rate of sand collected in each trap, and plotted as a function of distance from the shoreline in Figure 7 for the experiments listed in Table 1. The figure indicates that there are three distinct zones of transport; incipient breaking zone, inner surf zone, and swash zones.

Incipient Breaking Zone

At incipient breaking, a substantial peak in transport occurs for Test 3, the higher-energy plunging-wave case. However, an increase in transport is not observed in the other three cases. The absence of peak in transport for the spilling cases can be explained as a function of breaker type. Turbulence associated with spilling breakers remains close to the surface in the bore. The jet associated with the large plunging waves penetrated deep into the water column, impacting the bed, and caused sand to be suspended and transported by the longshore current (Wang et al., 2002b). It is interesting that a peak is not evident with Test 6. A possible explanation is that the approach slope to the breakpoint bar is much gentler than observed in Test 3, and the waves are weakly plunging. Further research will investigate the amount of sediment suspended, and thus made available for transport by longshore currents at the Test 6 breaker line.

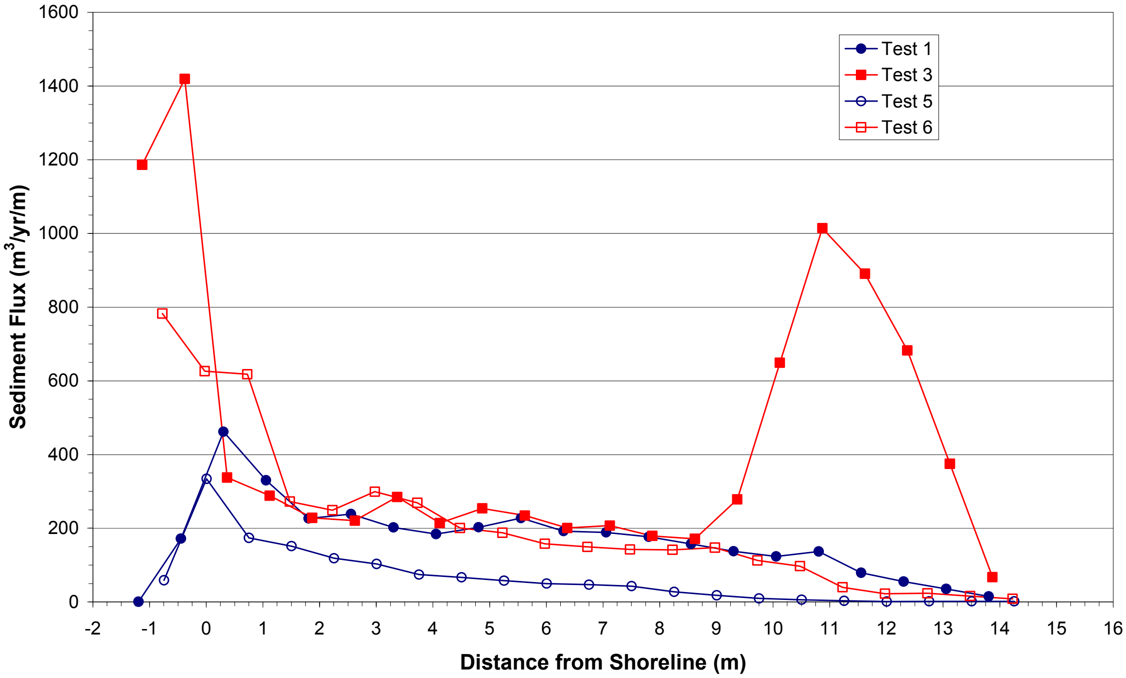

Fig. 7. Cross-shore distribution of measured longshore sediment transport

Inner Surf Zone

The inner surf zone shows that transport rates are approximately the same for three of the four cases. In the inner surf, energy is saturated and wave height is strongly controlled by depth. Depths in the inner surf zone are similar for all experiments, despite differences in incident wave height and period. Thus, it can be assumed that sediment flux is controlled solely by wave height in this zone for Tests 1, 3, and 6. It is not apparent why sediment flux measured during Test 5 is lower in the inner surf than the other three cases. However, Figure 4 shows that waves gradually decrease through the inner surf for Test 5, and not all waves were observed to break throughout the inner surf zone. Less wave breaking would produce less turbulence to suspend sand, and could possibly explain lower sediment flux for Test 5. Further research also will investigate the magnitude of bottom orbital velocities to determine the frequency at which critical shear stress is reached for Test 5.

Swash Zone

The swash zone was defined as the region where an increase in foreshore slope was observed increased, which was within 2 m from the shoreline for the present experiments. There is a peak in transport in the swash zone for all cases, and Figure 7 shows that swash zone transport has a dependence on wave period and height, with a stronger dependence on period. In most longshore sediment transport models the swash transport contribution is either completely ignored or merely accounted for as part of the total sediment transport budget (Van Wellen et al., 2000). However, significant swash zone transport rates have been observed in the field (Sawaragi and Deguchi, 1978, Bodge and Dean, 1987), and swash zone transport can account for up to 50 percent of the total longshore transport (Elfrink and Baldock, 2002, Van Wellen et al., 2000). For the higher energy cases (Test 1 and Test 3), swash zone transport accounts for 30 to 40 percent of the total transport. However, for the lower energy cases (Test 5 and Test 6), swash zone transport accounts for over 60 percent of the total transport. Additionally, the reduction in total transport between the higher and lower spilling cases (Test 1 and Test 5) was a factor of 2.8, but the reduction in swash transport was only 1.4. The reduction in total transport between higher and lower plunging cases (Test 3 and Test 6) was 2.2, but the reduction in swash zone transport was again only 1.4. Although data are limited, this implies that swash zone transport contributes more to the total transport rate for smaller scales, and conversely, as incident wave height increases the contribution of swash transport to total transport is less. The results indicate that the contribution of swash zone transport can be significant, and total longshore transport estimates should account for transport in this region.

In addition, results from the present study have implications to field measurements of longshore transport. Although swash zone transport measurements are difficult to obtain in the field, the results indicate that it is necessary to include swash zone transport to obtain accurate measurements of total longshore sediment transport. For example, if swash zone transport is neglected in the present study, the overestimates of the CERC formula increase by 50 to 250 percent.

SUMMARY

Measurements of longshore transport rates were performed in a large-scale physical model for four incident wave conditions that varied by breaker type and incident energy. Measured transport rates were compared to estimates computed using the CERC formula and Kamphuis (1991) equation. Additionally, the CERC formula, in particular the coefficient K, was evaluated. It was found that the CERC formula overestimated measurements by a factor of 7 to 8 for spilling breakers, and more than a factor of 3 for plunging breakers. The CERC formula is not sensitive to breaker type, which was found to be an important factor to total longshore transport rates. If the coefficient K of the CERC formula was calibrated using measured data and applied to similar breaker types, differences were reduced to 10 percent or less. Estimates using the Kamphuis equation, which includes wave period, that influences wave breaking, were good with differences ranging from 1 to 25 percent. The findings indicate that total longshore transport rate is a function of breaker type, and the CERC formula performs well if K is calibrated and applied to wave conditions having similar breaker type.

The cross-shore distribution of longshore sediment transport indicated three distinct zones of transport: the incipient breaker zone, the inner surf zone, and the swash zone. A peak in transport occurred for the higher energy plunging waves in the incipient breaker zone, indicating that the breaker type suspends more sediment for transport. Transport in the inner surf zone was near constant for three of the four wave conditions, indicating that energy is saturated and transport is controlled solely by depth. The exception was lower-energy spilling waves. Swash zone transport accounted for a significant percentage of the total transport, and future relationships should incorporate swash zone transport.

ACKNOWLEDGEMENTS

The authors wish to acknowledge William Halford, David Daily, and Tim Nisley who provided technical support for this study. The authors wish to thank Bruce Ebersole for review and thoughtful discussion on the paper. Ping Wang was jointly funded by the U.S Army Engineer Research and Development Center and the Louisiana Sea Grant College Program. Permission to publish this abstract was granted by the Headquarters, U.S. Army Corps of Engineers.

REFERENCES

Bodge, K.R. and Dean, R.G., 1987. Short-term impoundment of longshore transport, *Proceedings of Coastal Sediments '87*, 468-483.

Elfrink, B. and Baldock, T. 2002. Hydrodynamics and sediment transport in the swash zone: a review and perspectives, *Coastal Engineering*, 45, 149-167.

Fowler, J.E.; Rosati, J.D.; Hamilton, D.G., and Smith, J.M., 1995. Development of a large-scale laboratory facility for longshore sediment transport research. *The CERCular, CERC-95-2*, U.S. Army Engineer Waterways Experiment Station, Vicksburg, MS.

Galvin, C.J., 1968. Breaker type classifications of three laboratory beaches, *Journal of Geophysical Research*, 73, 3651-3659.

Hamilton, D.G., Ebersole, B.A., Smith, E.R., and Wang, P., 2001. Development of a Large-Scale Laboratory Facility for Sediment Transport Research. *Technical Report*, U.S. Army Engineer Research and Development Center, Vicksburg, MS.

Hamilton, D.G., and Ebersole, B.A., 2001. Establishing Uniform Longshore Currents in a Large-Scale Laboratory Facility. *Coastal Engineering*, 42, 199-218.

Johnson, B. D. 2003. Nearhyds, Nearshore hydrodynamics, steady U. S. Army Engineer Research and Development Center, Vicksburg, Mississippi, in press.

Kamphuis, J.W., 1991. Alongshore sediment transport rate. *Journal of Waterways, Port, Coastal and Ocean Engineering*, ASCE, 117(6), 624-641.

Kamphuis, J.W., 2002. Alongshore transport of sand, *Proceedings of the 28th Coastal Engineering Conference*, ASCE, in press.

Komar, P.D. and Inman, D.L., 1970. Longshore sand transport on beaches. *Journal of Geophysical Research,* 75(30), 5514-5527.

Kraus, N.C.; Isobe, M.; Igarashi, H.; Sasaki, T.O., and Horikawa, K., 1982. Field experiments on longshore transport in the surf zone, *Proceedings of the 18th Conference on Coastal Engineering*, ASCE, 969-988.

Kraus, N.C. and Larson, M., 1991. NMLONG: Numerical model for simulating the longshore current – Report 1: model development and tests. *Technical Report DRP-91-1*, U.S. Army Engineer Waterways Experiment Station, Vicksburg, Mississippi.

Miller, H.C., 1998. Comparison of storm longshore transport rates to predictions, *Proceedings of the 26th Conference on Coastal Engineering*, ASCE, 2954-2967.

Sawaragi, T. and Deguchi I., 1978. Distribution of sand transport rate across the surf zone, *Proceedings of the 16th Conference on Coastal Engineering*, ASCE, 1596-1613.

Schoonees, J.S. and Theron, A.K., 1993. Review of the field data base for longshore sediment transport. *Coastal Engineering*, 19, 1-25.

Schoonees, J.S. and Theron, A.K., 1994. Accuracy and applicability of the SPM longshore transport formula. *Proceedings of the 24th Coastal Engineering Conference*, ASCE, 2595-2609.

Shore Protection Manual, 1984. U.S. Army Corps of Engineers, Coastal Engineering Research Center, U.S. Government Printing Office, Washington, D.C.

Sunamura, T., and Kraus, N. C. 1985. Prediction of average mixing depth of sediment in the surf zone. *Marine Geology*, 62, 1-12.

Van Wellen, E., Baldock, T., Chadwick, A., and Simmonds, D., 2000. STRAND – a model for longshore sediment transport in the swash zone, *Proceedings of the 27th Conference on Coastal Engineering*, ASCE, 3139-3150.

Visser, P.J., 1991. Laboratory measurements of uniform longshore currents. *Coastal Engineering*, 15, 563-593.

Wang, P.; Kraus, N.C., And Davis, R.A., Jr., 1998. Total rate of longshore sediment transport in the surf zone: field measurements and empirical predictions. *Journal of Coastal Research*, 14(1), 269-283.

Wang, P. and Kraus, N.C., 1999. Longshore sediment transport rate measured by short-term impoundment. *Journal of Waterway, Port, Coastal & Ocean Engineering*, ASCE, 125, 118-126.

Wang, P., Smith, E.R., and Ebersole, B.A., 2002a. Large-scale laboratory measurements of longshore sediment transport under spilling and plunging breakers. *Journal of Coastal Research*, 18(1), 118-135.

Wang, P., Ebersole, B.A., Smith, E.R., and Johnson, B.D., 2002b. Temporal and spatial variations of surf-zone currents and suspended sediment concentration. *Coastal Engineering*, (46), 175-211.